

From d - to p -wave pairing in the $t-t'$ Hubbard model at zero temperature

R. Arita and K. Held

Max-Planck-Institut für Festkörperforschung, 70569 Stuttgart, Germany

(Dated: December 2, 2024)

We develop a DCA(PQMC) algorithm which employs the projective quantum Monte Carlo (PQMC) method for solving the equations of the dynamical cluster approximation (DCA) at zero temperature, and apply it for studying pair susceptibilities of the two-dimensional Hubbard-model with next-nearest neighbor hopping. In particular, we identify which pairing symmetry is dominant in the U - n parameter space (U : repulsive Coulomb interaction; n : electron density). We find that p_{x+y} - ($d_{x^2-y^2}$ -) wave is dominant among triplet (singlet) pairings -at least for $0.3 < n < 0.8$ and $U \leq 4t$. The crossover between $d_{x^2-y^2}$ -wave and p_{x+y} -wave occurs around $n \sim 0.4$.

PACS numbers: 71.27.+a, 71.10.Fd

Since the discovery of high-temperature superconductivity [1] the purse of identifying the microscopic mechanism for unconventional superconductivity such as d -wave in cuprates or p -wave in ruthenates has been a main driving force in condensed matter physics. Even now, 19 years after the discovery of high-temperature superconductivity, it is an issue of hot debate whether the one-band (two-dimensional) Hubbard model, the simplest model for electronic correlations, is becoming d -wave or -further away from half-filling- p -wave superconducting at low temperatures.

There are indications that there is indeed $d_{x^2-y^2}$ -wave superconductivity close to half-filling [2]. For example, the functional renormalization group (fRG) predicts superconductivity for weak coupling [3]. Also numerical quantum Monte Carlo (QMC) simulations for finite size systems [4] observe an enhancement of the $d_{x^2-y^2}$ -wave pairing. A promising method for addressing these questions is the dynamical cluster approximation (DCA) [5], an extension of dynamical mean field theory (DMFT) [6], which also takes non-local correlations and wave-vector dependences into account. This is essential for describing p - and d -wave superconductivity; DMFT itself only allows for s -wave superconductivity by construction. Such DCA calculations [7] find $d_{x^2-y^2}$ -wave superconductivity. However, when solving the DCA equations numerically by conventional Hirsch-Fye QMC simulations [8] one is restricted to rather high temperatures T [7, 9]. Hence, a difficult extrapolation to low T is necessary which is further hampered since (numerically) exact statements also require an extrapolation cluster size $N_c \rightarrow \infty$.

Our paper will focus on a different parameter regime: Motivated by Sr_2RuO_4 , many authors have recently addressed the possibility of triplet superconductivity in the two-dimensional one-band Hubbard model with finite next nearest neighbor hopping t' (the $t-t'$ Hubbard model) at intermediate electron densities. The results have been controversial as regards the dominant pairing symmetry: fRG calculations [10, 11, 12] concluded that when $t' > 0.3t - 0.4t$ and the Fermi level is at the van Hove (vH) singularity, the system becomes ferro-

magnetic at sufficiently low T . While a d -wave phase spreads next to the ferromagnetic phase in the $U-t'$ diagram for vH band fillings, a p -wave phase exists when going away from the vH band filling and for sufficiently large t' . Third-order perturbation theory [14] showed that triplet superconductivity is realized even when ferromagnetic spin fluctuation are not dominant. On the other hand, QMC [13], FLEX [13], and DCA [9] calculations concluded that triplet pairing does not become dominant for intermediate filling even when t' is as large as $0.4t$.

It should be noted that fRG, third-order perturbation theory and the FLEX approximation are valid only for weak coupling; finite-size QMC is possible only for $U < 2t$ because of a serious negative sign problem [13]; and the DCA has been performed only for high T s [9]. Thus, the question concerning p -wave (triplet) superconductivity in the Hubbard model is not conclusive yet.

In this paper, we introduce a new route to address this question, solving the DCA equations by an extended version of the projective QMC (PQMC) method [15]. This DCA(PQMC) approach mitigates the T -extrapolation problem of DCA(QMC). We concentrate on the crossover between d - and p -wave instability in the intermediate electron density range $0.3 \lesssim n \lesssim 0.8$ and present results for the paramagnetic spectral function and the dominant pairing symmetry for $U \lesssim 4t$ and $t' = 0.4t$. On an equal footing with these pair susceptibilities, we also calculate the ferromagnetic and antiferromagnetic spin susceptibility of the DCA cluster.

DCA(PQMC) method. The $t-t'$ Hubbard model reads

$$H = -t \sum_{i,j,\sigma}^{\text{NN}} c_{i\sigma}^\dagger c_{j\sigma} + t' \sum_{i,j,\sigma}^{\text{NNN}} c_{i\sigma}^\dagger c_{j\sigma} + U \sum_i n_{i\uparrow} n_{i\downarrow}. \quad (1)$$

Here, $c_{i\sigma}^\dagger$ and $c_{i\sigma}$ create and annihilate an electron with spin σ on site i of the two-dimensional lattice; the first and second sum are restricted to nearest neighbors (NN) and next-nearest neighbors (NNN), respectively. In the following, all energies are given in units of t , corresponding to a bandwidth of $D = 8(t)$.

In the DCA [5], the Brillouin zone is divided into N_c patches, with a coarse-grained Green function $\bar{G}(\mathbf{K}_p, \omega)$ and self energy $\Sigma_c(\mathbf{K}_p, \omega)$ for every patch p :

$$\bar{G}(\mathbf{K}_p, \omega) = \frac{N_c}{N} \sum_{\tilde{\mathbf{k}}} \left[G_0^{-1}(\mathbf{K}_p + \tilde{\mathbf{k}}) - \Sigma_c(\mathbf{K}_p, \omega) \right]^{-1}. \quad (2)$$

Here, G_0^{-1} is the non-interacting Green function and the $\tilde{\mathbf{k}}$ summation averages over all \mathbf{k} -points of patch p which is centered around \mathbf{K}_p ; N is the total number of all \mathbf{k} -points. \bar{G} and Σ_c then define an effective cluster of Anderson impurities which can be described by the non-interacting Green function $\mathcal{G}_0(\mathbf{K}_p, \omega)^{-1} = \bar{G}(\mathbf{K}_p, \omega)^{-1} + \Sigma_c(\mathbf{K}_p, \omega)$, or its Fourier transform $\mathcal{G}_0(\omega) \mathbf{x}_i \mathbf{x}_j$. This defines a cluster problem H_c given by $\mathcal{G}_0(\omega) \mathbf{x}_i \mathbf{x}_j$ and a local Coulomb interaction on every cluster site X_i . In the DCA, this cluster problem has to be solved self-consistently together with Eq. (2).

Here, we introduce a new cluster solver which is based on PQMC [15] and particularly constructed for zero temperature. Just as in [15], $T = 0$ expectation values of an arbitrary operator \mathcal{O} are calculated as:

$$\langle \mathcal{O} \rangle_0 = \lim_{\theta \rightarrow \infty} \lim_{\tilde{\beta} \rightarrow \infty} \frac{\text{Tr} \left[e^{-\tilde{\beta} H_T} e^{-\theta H_c/2} \mathcal{O} e^{-\theta H_c/2} \right]}{\text{Tr} \left[e^{-\tilde{\beta} H_T} e^{-\theta H_c} \right]}.$$

where H_T is an auxiliary Hamiltonian for which we take the cluster defined by $\mathcal{G}_0(\omega) \mathbf{x}_i \mathbf{x}_j$ without Coulomb interaction ($U = 0$). The local one-particle potential of H_T is adjusted self-consistently to yield the same n as the interacting cluster H_c . At least for $N_c = 1$, this yields the same asymptotic behavior of $\mathcal{G}_0(\tau)$ and $\bar{G}(\tau)$ for large τ . Hence, the influence of breaking time translational symmetry at $\tau = \theta$ is reduced. This gives a smoother Green function in the vicinity of $\tau = \theta$, but does not affect the results after long enough projection, i.e., sufficiently away from $\tau = \theta$.

As in [15], the limit $\tilde{\beta} \rightarrow \infty$ can be taken analytically for this H_T . Then, the interacting Green function G is obtained via the same updating equations for the auxiliary Hubbard-Stratonovich fields as for finite- T QMC. But the PQMC starting point is different: a $T = 0$ Green function with open boundary conditions defined for $0 \leq \tau, \tau' \leq \theta = 16t, 18t$, discretized into $L = 48, 64$ slices for $N_c = 4 \times 4 = 16$ cluster sites. For the measurement of physical quantities, $\mathcal{L} = 8, 10, 12$ central time slices are taken, and the remaining \mathcal{P} time slices on the right and left side of the measuring interval are reserved for projection. Typically, we performed 10^5 to 6×10^5 QMC sweeps. To obtain $G(i\omega)$ from $G(\tau)$, the maximum entropy method (MEM) is employed, as in [15].

Spectral properties of the paramagnetic phase. Now, let us turn to the DCA(PQMC) results. We performed calculations for $n = 0.3, 0.4, 0.6, 0.8$ and $U = 2t, 3.5t, 4t$. Throughout the study, we took $t' = 0.4t$ and $N_c =$

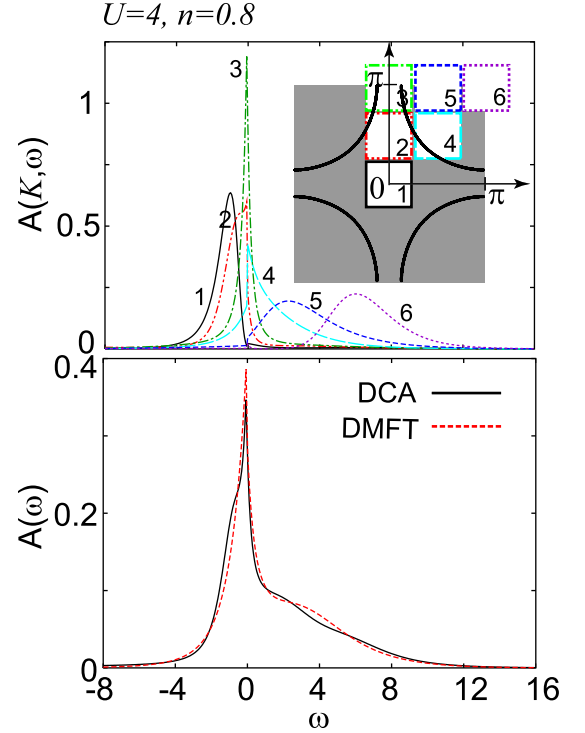


FIG. 1: (Color online) Top panel: Spectral function $A(K_p, \omega)$ for $U = 4t, n = 0.8$ and the 6 (out of 16) irreducible patches p indicated in the inset. The inset also shows the non-interacting Fermi surface as a line. Bottom panel: \mathbf{k} -integrated spectral function $A(\omega)$ compared with that of DMFT.

$4 \times 4 = 16$ DCA patches. In the upper panel of Fig. 1, we present the one-particle spectral function $A(\mathbf{K}_p, \omega) = -1/\pi \text{Im} \bar{G}(\mathbf{K}_p, \omega)$, i.e., the averaged spectrum over the six irreducible patches p of the Brillouin zone, as indicated in the inset. Patches 2, 3, and 4 have contributions at the Fermi surface and hence a contribution at $\omega = 0$. Thereby, $A(\mathbf{K}_3, \omega)$ has a particular sharp peak because the vH singularity is located at $(\pi, 0)$ and $(0, \pi)$. This sharp peak also reflects in the fully \mathbf{k} -integrated $A(\omega) = \sum_p A(\mathbf{K}_p, \omega)$, shown in the bottom panel of Fig. 1. Let us note that the quantitative and qualitative features are very similar to those of DMFT (dashed line); there is no pseudo gap for $t' = 0.4, n = 0.8, U = 4t$ in our $T = 0$ DCA(PQMC) calculation.

Calculation of cluster susceptibilities. To discuss the magnetic and pairing instabilities, we first calculate the corresponding susceptibilities

$$\chi^{\text{spin}}(\mathbf{Q}, \tau_1 - \tau_2) = \sum_{\mathbf{X}_1, \mathbf{X}_2} e^{i\mathbf{Q}(\mathbf{X}_1 - \mathbf{X}_2)} \langle T_\tau c_{\mathbf{X}_1 \uparrow}^\dagger(\tau_1) c_{\mathbf{X}_1 \downarrow}(\tau_1) c_{\mathbf{X}_2 \downarrow}^\dagger(\tau_2) c_{\mathbf{X}_2 \uparrow}(\tau_2) \rangle, \quad (3)$$

$$\chi^{\text{pair}}(\tau_1 - \tau_2) = \sum_{\mathbf{X}_1, \mathbf{X}_2} g(\mathbf{K}_1) g(\mathbf{K}_2) \langle T_\tau c_{\mathbf{K}_1 \uparrow}(\tau_1) c_{-\mathbf{K}_1 \downarrow}(\tau_1) c_{-\mathbf{K}_2 \downarrow}^\dagger(\tau_2) c_{\mathbf{K}_2 \uparrow}^\dagger(\tau_2) \rangle \quad (4)$$

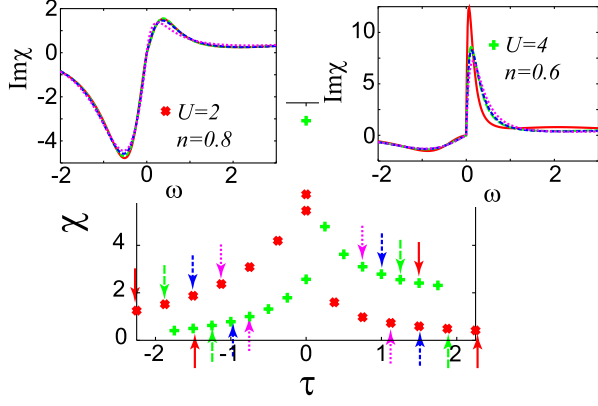


FIG. 2: (Color online) Susceptibilities for $d_{x^2-y^2}$ -wave pairing in τ -space for $U=2t, n=0.8$ (crosses) and $U=4t, n=0.6$ (circles). The arrows indicate different cutoffs τ_c up to which $\chi(\tau)$ information was taken into account in MEM for obtaining the $\text{Im}\chi(\omega)$ of the insets (dotted, dashed, long dashed, and solid line are for the corresponding $\tau_c \downarrow$ of the main figure). For $U=2t, n=0.8$ (left inset), the result is basically τ_c -independent; but for $U=4t, n=0.6$ (right inset) the peak at small ω is largely enhanced if τ_c is increased.

for the 4×4 cluster at self-consistency. Here, $c_{\mathbf{K}\sigma} = \sum_{\mathbf{X}} c_{\mathbf{X}\sigma} \exp(i\mathbf{K}\mathbf{X})$ and $g(\mathbf{K})$ is the form factor, i.e., $g(\mathbf{K})=1$ for s -wave, $\sqrt{2} \sin(K_x)$ for p_x wave, $\sqrt{2} \sin(K_x + K_y)$ for p_{x+y} wave, $\cos(K_x) - \cos(K_y)$ for $d_{x^2-y^2}$ wave. Second, we calculate $\text{Im}\chi(\omega)$ from $\chi(\tau)$ by MEM and from this obtain the static susceptibility via the Kramers-Kronig relation $\chi(\omega=0) = \int \text{Im}\chi(\omega)/\omega d\omega$.

In DCA, the susceptibilities of the Hubbard model are calculated from the above cluster χ by solving the Bethe-Salpeter equation [5]. However, to this end it would be necessary to calculate susceptibilities for two τ 's instead of Eqs. (3) and (4) which would tremendously increase the numerical effort. Hence, we look at the cluster susceptibilities Eqs. (3) and (4) for simplicity. We can expect that this quantity already captures the essential features of the competition between ferromagnetic and antiferromagnetic spin fluctuation, or that between superconductivity with different symmetries.

Let us mention one more technical point: The decay of χ in τ -space can be underestimated because of a finite number of projection time slices \mathcal{P} . In this case, the MEM calculation of $\text{Im}\chi(\omega)$ depends on up to which τ_c value the MEM input $\chi(\tau)$ is considered, see Fig. (2). Whenever we encounter a strong cutoff (τ_c -)dependence like in Fig. 2 (right inset) we take a short cutoff τ_c (only four τ points). With such a short cutoff τ_c which is very close to the asymptotical behavior $\tau_c \rightarrow 0$, we certainly do not overestimate $\chi(0)$. However, if the weak decay of χ in τ -space is not due to the finite \mathcal{P} but due to physics, we *underestimate* $\chi(0)$ this way. In Figs. 3 and 4, these more problematic data points, where we possibly *underestimate* $\chi(0)$, are indicated by an arrow.

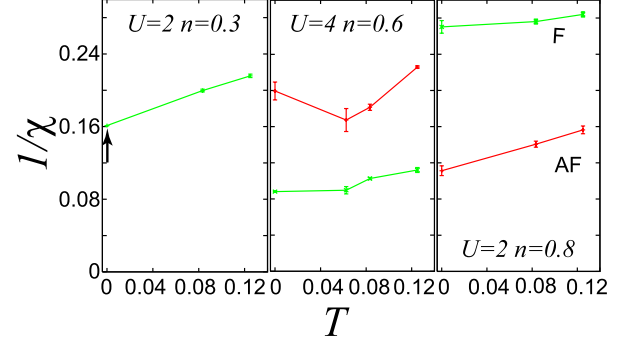


FIG. 3: (Color online) Inverse magnetic susceptibilities as a function of T for $U = 2t, n = 0.3$ (left), $U = 4t, n = 0.6$ (middle), and $U = 2t, n = 0.8$ (right). The arrows indicate those data points where χ is possibly underestimated ($1/\chi$ overestimated), as discussed in Fig. 2.

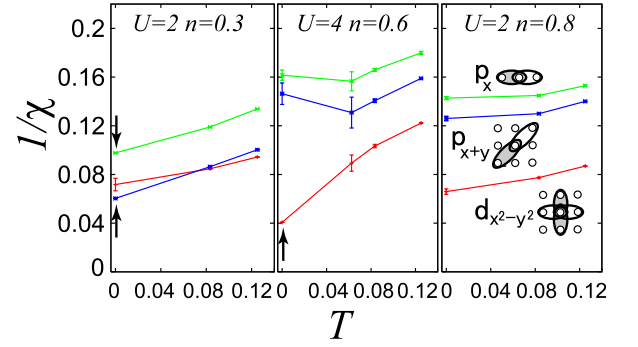


FIG. 4: (Color online) Same as Fig. 3, but now for p_x , p_{x+y} , and $d_{x^2-y^2}$ -wave pairing as indicated in the right panel.

Instabilities of the paramagnetic phase. Let us finally turn to the physical results, starting with the (inverse) ferromagnetic and antiferromagnetic susceptibilities plotted in Fig. 3 as a function of T for three exemplary parameter values; finite- T data have been obtained by conventional DCA(PQMC). First of all, let us emphasize the obvious: DCA(PQMC) directly provides well for the $T=0$ susceptibilities *without* extrapolation -in very contrast to the finite- T DCA(QMC) for which it is difficult to forecast/extrapolate the low- T behavior. Turning to the physical results, we see that the ferromagnetic spin susceptibility becomes larger than the antiferromagnetic one for $n \leq 0.6$. Note that the vH filling is at ~ 0.6 for $t' = 0.4$. In fact, the fRG studies [11, 12] found a strong ferromagnetic instability for $t' > 0.3 \sim 0.4$ at vH band fillings. Thus, the qualitative tendency of our results and those of the fRG studies are consistent.

Next, let us discuss superconductivity. Fig. 4 shows the inverse static pair susceptibilities as a function of T . First of all, we find that $d_{x^2-y^2}$ -wave (p_{x+y} -wave) is dominant among singlet (triplet) pairings for all (U, n) 's considered. For $n=0.8$, $d_{x^2-y^2}$ -wave dominates over triplet pairings

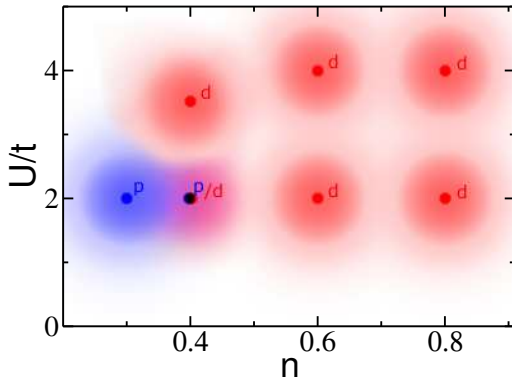


FIG. 5: (Color online) U - n diagram showing the dominant pairing symmetry; for $n = 0.4$, $U = 2t$ it is too close to call which instability is strongest.

as expected. When we reduce n to 0.6, antiferromagnetic spin fluctuation become weak, see Fig. 3. Nonetheless, the $d_{x^2-y^2}$ -wave instability is still larger than those for triplet pairings. This is consistent with finite temperature DCA calculation for $U = 3t$, $n = 0.67$ [9], and suggests $d_{x^2-y^2}$ -wave ordering for low enough T -even for far away from half-filling. These findings are also in accord with QMC calculations for a finite-size Hubbard model [13], showing a dominant $d_{x^2-y^2}$ -wave instability for $t' \sim 0.4$, $n \sim 0.67$, and $U = 2t$. The fRG [12] reports also a ferromagnetic phase for $t' = 0.4$, $n \sim 0.6$, and $U > t$, while there is possibly a d -wave phase for $U < t$. On the other hand, third ordered perturbation calculations [14] have shown that triplet superconductivity becomes dominant even for weak coupling. We find such triplet pairing only for smaller n 's, while the detailed structure of \mathbf{k} -dependence of the vertex corrections may be essential which is possibly smeared out by the coarse-graining of DCA.

Discussion and Outlook. Fig. 5 summarizes our main finding, i.e., the dominant superconducting susceptibility on the cluster. We find that $d_{x^2-y^2}$ -wave pairing is dominant in an unexpectedly broad range of fillings n , whereas p_{x+y} -wave prevails only for small n . The transition between p_{x+y} -wave and $d_{x^2-y^2}$ -wave is at about $n \sim 0.4$.

The $t-t'$ Hubbard model with $t' \sim 0.4$ and $n \sim 2/3$ has been considered to be a good model for the γ -band of Sr_2RuO_4 [14]. Our DCA(PQMC) results indicate however that there is no triplet superconductivity for these n and t' values, at least for the moderately strong values of U we studied and which are e.g. considered in local density approximation (LDA)+DMFT calculations [17].

Hence our results suggest that a nearest-neighbor Coulomb interaction V [9] or a multi-orbital model

is necessary for an appropriate description of triplet pairing in Sr_2RuO_4 below $T_c \sim 1$ K. In contrast to the standard finite- T DCA(QMC), we can expect that DCA(PQMC) will open the door to such low temperatures -even for calculations with orbital realism. Similarly, we can hope that DCA(PQMC) will allow for more definite statements concerning superconductivity in the two-dimensional Hubbard model in the future. To this end, still a $N_c \rightarrow \infty$ extrapolation and the calculation of lattice susceptibilities is necessary. But at least the problematic extrapolation to low temperatures is mitigated; PQMC is the direct route to $T=0$.

We acknowledge discussions with M. Feldbacher and A. A. Katanin as well as support by the Alexander von Humboldt foundation (RA) and the Emmy Noether program of the Deutsche Forschungsgemeinschaft (KH).

- [1] J. G. Bednorz and K. A. Müller, *Z. Phys. B* **64**, 189 (1986).
- [2] D. J. Scalapino, *Phys. Rep.* **250**, 329 (1995).
- [3] D. Zanchi and H. J. Schulz, *Phys. Rev. B* **54**, 9509 (1996); **61**, 13609 (2000); C. J. Halboth and W. Metzner, *Phys. Rev. B* **61**, 7364 (2000); C. Honerkamp *et al.*, *Phys. Rev. B* **63**, 35109 (2001).
- [4] S. R. White *et al.*, *Phys. Rev. B* **39**, 839 (1989); *Phys. Rev. B* **40**, 506 (1989); K. Kuroki and H. Aoki, *Phys. Rev. B* **56**, R14287 (1997).
- [5] M. H. Hettler *et al.*, *Phys. Rev. B* **58**, (1998) 7475; T. A. Maier *et al.*, cond-mat/0404055. A. I. Lichtenstein and M. I. Katsnelson, *Phys. Rev. B* **62**, R9283 (2000); An alternative cluster DMFT approach has been proposed by G. Kotliar *et al.*, *Phys. Rev. Lett.* **87**, 186401 (2001).
- [6] W. Metzner and D. Vollhardt, *Phys. Rev. Lett.* **62**, 324 (1989); A. Georges *et al.*, *Rev. Mod. Phys.* **68**, 13 (1996); G. Kotliar and D. Vollhardt, *Physics Today* **57**, 53 (2004).
- [7] T. A. Maier *et al.*, cond-mat/0504529.
- [8] J. E. Hirsch and R. M. Fye, *Phys. Rev. Lett.* **56**, 2521 (1986).
- [9] R. Arita *et al.*, *Phys. Rev. Lett.* **92**, 247006 (2004).
- [10] C. Honerkamp and M. Salmhofer, *Phys. Rev. Lett.* **87**, 187004 (2001); *Phys. Rev. B* **64**, 184516 (2001).
- [11] C. Honerkamp *et al.*, *Phys. Rev. B* **70**, 235115 (2004).
- [12] A. A. Katanin and A. P. Kampf, *Phys. Rev. B* **68**, 195101 (2003).
- [13] K. Kuroki *et al.* *Phys. Rev. B* **69**, 214511 (2004).
- [14] T. Nomura and K. Yamada, *J. Phys. Soc. Jpn.* **69**, 3678 (2000).
- [15] M. Feldbacher, K. Held, and F. F. Assaad, *Phys. Rev. Lett.* **93**, 136405 (2004); for a multi orbital extension see R. Arita and K. Held, cond-mat/0504040.
- [16] M. Jarrell *et al.*, *Phys. Rev. B* **64**, 195130 (2001).
- [17] A. Liebsch and A. I. Lichtenstein, *Phys. Rev. Lett.* **84**, 1591 (2000).